ELSEVIER

Higher trapped field over 5 T on HTSC bulk by modified pulse field magnetizing

Hiroyuki Fujishiro [a,*], Tatsuya Tateiwa [a], Atsushi Fujiwara [a],
Tetsuo Oka [b], Hidemi Hayashi [c]

[a] *Iwate University, 3-4-5 Ueda, Morioka 020-8551, Japan*
[b] *IMRA Material R&D Co., Ltd., 5-50 Hachiken-cho, Kariya 448-0021, Japan*
[c] *Kyushu Electric Power Co., Inc., 2-1-47 Shiobaru, Fukuoka 815-8520, Japan*

Abstract

The trapped field $B_T^P = 5.20$ T has been realized on the GdBaCuO bulk superconductor by a modified multi pulse technique combined with a stepwise cooling (MMPSC), which surpassed the previous highest record of $B_T^P = 4.47$ T. At the first stage, a small amount of the magnetic field ~ 1 T was trapped at the bulk center with a concave field distribution at a high starting temperature $T_s \sim 45$ K by the low pulse field application $B_{ex} \sim 4.5$ T. Following the first stage, the higher field of $B_{ex} \sim 6.7$ T was applied at a lower $T_s \sim 30$ K at the second stage. The concave trapped field profile over the bulk at the first stage and the optimization of the higher applied pulse field at the second stage are key points to enhance B_T above 5 T.
© 2006 Elsevier B.V. All rights reserved.

1. Introduction

The pulse field magnetizing (PFM) on high-T_c bulks has been recently intensively investigated instead of the field cooled magnetizing (FCM) because of the relatively compact, inexpensive and mobile setup [1]. However, the trapped field B_T^P by PFM had been pretty smaller than that attainable by FCM at low temperatures possibly due to the large temperature rise ΔT by the dynamical motion of the magnetic flux. The highest B_T^P value ever reported had been 3.80 T on the SmBaCuO bulk at 30 K by an improved iterative pulse field magnetization method with reduced amplitude (IMRA) [2]. We have systematically measured the time evolution of the temperature rise $\Delta T(t)$ on the surface of the cryo-cooled REBaCuO bulks during the PFM and

investigated the relation between ΔT and B_T^P [3–5]. The heat generation results from both the pinning loss Q_p related to the flux trapping and the viscous loss Q_v related to the flux movement. The successive pulses with the same strength make the ΔT value decrease and the B_T^P value increase with increasing number of the pulse application. The lowering of the bulk starting temperature T_s is expected to result in a higher B_T^P due to the enhanced pinning force F_p but it also brings about a larger ΔT due to an increase of Q_p and a decrease of the specific heat $C(T)$. As a result, B_T^P at $T_s = 10$ K was not enhanced contrary to our expectation [6]. Recently, we proposed a new PFM technique named as a modified multi-pulse technique combined with a stepwise cooling (MMPSC) [7]. This technique consists of two stages; firstly, a small amount of magnetic field ($B_T^P \sim 1$ T) is trapped in the bulk center by applying a lower field $B_{ex}(1) \sim 4.5$ T at a higher temperature $T_s(1) \sim 45$ K, realizing a concave trapped field distribution over the bulk

sample. Secondly, the bulk is cooled down to $T_s(2) \sim 30$ K and the higher pulse fields of $B_{ex}(2) \sim 6.7$ T are applied twice. As a result, we obtained $B_T^P = 4.47$ T on the surface of the GdBaCuO bulk, which was the highest record using PFM technique at that time [8]. The reduction of ΔT due to the already trapped flux at the first stage and the application of the higher $B_{ex}(2)$ at the second stage are key points to enhance B_T^P.

In this paper, we inquire into this technique and report the renewed highest B_T^P value of 5.20 T by the MMPSC technique. We elucidate the importance of the optimization of $B_{ex}(2)$ at the second stage and investigate the effect of the stainless steel ring set onto the bulk disk on the B_T^P value.

2. Experimental

A highly c-axis oriented GdBaCuO bulk disk (45 mm in diameter and 15 mm in thickness, Nippon Steel Co., Ltd.) was used. The experimental setup around the bulk is shown in the inset of Fig. 1(a). The stainless steel ring with 4 mm in thickness and 15 mm in height was tightly set onto the bulk disk using Apiezon-N grease in order to reduce ΔT during PFM [8]. The bulk with the ring was stacked on the soft-iron disk on the cold stage of the GM cycle helium refrigerator and was magnetized using a solenoid-type pulse coil dipped in liquid N_2 with a soft-iron cylinder [7]. Three Hall sensors (F.W. Bell, model BHA 921) were

adhered to the position C (bulk center), M (8 mm distant from the bulk center) and E (16 mm distant from the bulk center) and the time evolutions of the local fields [$B_L(C)(t)$, $B_L(C)(t)$ and $B_L(E)(t)$] were monitored on a digital oscilloscope. The applied field $\mu_0 H_a(t)$, of which the maximum strength was defined as B_{ex}, was monitored by the current $I(t)$ flowing through the shunt resistor. The rising time of the pulse field was 13 ms and the duration was $\sim$80 ms. The bulk temperature $T(t)$ was measured at the position T using a fine thermocouple.

3. Results and discussion

We have performed three MMPSC runs (RUN-1– RUN-3). Table 1 summarizes the initial conditions [T_s and B_{ex}] and the results [T_{max}, ΔT_{max} and $B_T(C)$] for each run, where B_T^P means B_L ($t \to \infty$). For RUN-1, at the first stage, the pulse field of $B_{ex}(1) = 4.8$ T was applied twice (pulse No. 1 and No. 2) at $T_s(1) = 47$ K. Then the bulk was cooled down to $T_s(2) \sim 28$ K and the higher $B_{ex}(2) \sim 6.7$ T was applied twice at the second stage (pulse No. 3 and No. 4). The highest $B_T^P = B_T(C) = 5.20$ T was attained for the pulse No. 4. The first stage procedure of RUN-2 and RUN-3 was performed under the similar conditions to that of RUN-1 and, for the second stage, the higher $B_{ex}(2)$ (=7.01 T for RUN-2) and lower $B_{ex}(2)$ (=6.04 T for RUN-3) were applied in order to clarify the importance of the strength of $B_{ex}(2)$. In Table 1, the initial conditions and the results using the same bulk without the stainless steel ring are also shown as RUN-0, in which $B_T^P = 4.47$ T was obtained [7].

Figs. 1(a) and (b) show the time dependences of the applied field $\mu_0 H_a(t)$ and the local fields [$B_L(C)(t)$, $B_L(M)(t)$, $B_L(E)(t)$] for RUN-1 after applying the pulse No. 1 and No. 3, respectively. $B_L(E)(t)$, $B_L(M)(t)$, and $B_L(C)(t)$ rise up in this order, take a maximum and then slowly decrease to a final stable value. The maximum value of $B_L(E)(t)$ is 4.0 T but that of $B_L(C)(t)$ reaches only about 0.9 T. The maximum temperature rise ΔT_{max} (=18 K) takes place, which may mainly come from the heat generation due to the flux trapping. For the pulse No. 2, the maximum of $B_L(E)(t)$ decreases to 2.9 T and ΔT_{max} also decreases to 5 K due to the already trapped fluxes which obstruct the intrusion of the magnetic flux. $B_T(C)$ shows a slight increase to 1.10 T but the $B_T(M)$ and $B_T(E)$ are nearly unchanged, both of which are higher than $B_T(C)$. For the pulse No. 3 as shown in Fig. 1(b), the maximum of $B_L(E)(t)$ remains at 4.2 T, while that of $B_L(C)(t)$ increases to 6.0 T and $B_T^P = B_T(C)$ survives at 5.12 T. These results come from the ΔT reduction due to the trapped fluxes during the first stage and the small ΔT_{max} (=29 K) and low T_{max} (=57 K) prevent the escape of the magnetic fluxes from the bulk. For the pulse No. 4, $B_T^P = B_T(C)$ slightly increases to 5.20 T.

Figs. 2(a) and (b) present the time evolution of the local field $B_L(t)$ as a function of the distance along the radius direction on the bulk for the pulse No. 1 of RUN-1 for
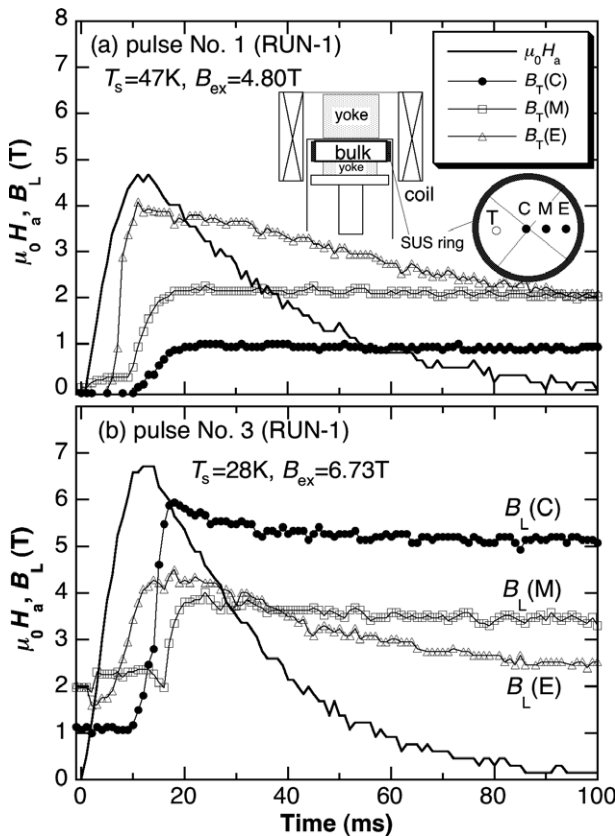

Fig. 1. The applied field [$\mu_0 H_a(t)$] and the local fields [$B_L(C)(t)$, $B_L(C)(t)$, $B_L(E)(t)$] for RUN-1 after applying the (a) pulse No. 1 and (b) pulse No. 3.

Table 1
The initial conditions [T_s, B_{ex}] and the results [T_{max}, ΔT_{max}, final B_T^P] of three MMPSC runs; the RUN-0 shows the previous results in which $B_T^P = 4.47$ T was attained [7]

| Run		First stage		Second stage		Final B_T^P
		Pulse No.1	Pulse No. 2	Pulse No. 3	Pulse No. 4	
RUN-1	$T_s(B_{ex})$	47 K (4.80 T)	47 K (4.80 T)	28 K (6.73 T)	28 K (6.56 T)	
	$T_{max}(\Delta T_{max})$	65 K (18 K)	52 K (5 K)	**57 K (29 K)**	50 K (22 K)	**5.20 T**
RUN-2	$T_s(B_{ex})$	47 K (4.80 T)	48 K (4.94 T)	27 K (7.01 T)	29 K (6.72 T)	
	$T_{max}(\Delta T_{max})$	65 K (18 K)	52 K (4 K)	**59 K (32 K)**	53 K (24 K)	**3.02 T**
RUN-3	$T_s(B_{ex})$	46 K (4.52 T)	46 K (4.52 T)	29 K (6.04 T)	30 K (6.87 T)	
	$T_{max}(\Delta T_{max})$	64 K (18 K)	50 K (4 K)	**49 K (20 K)**	52 K (22 K)	**4.10 T**
RUN-0	$T_s(B_{ex})$	45 K (4.54 T)	48 K (4.60 T)	29 K (6.72 T)	29 K (6.59 T)	
	$T_{max}(\Delta T_{max})$	62 K (18 K)	53 K (5 K)	**58 K (29 K)**	53 K (24 K)	**4.47 T**
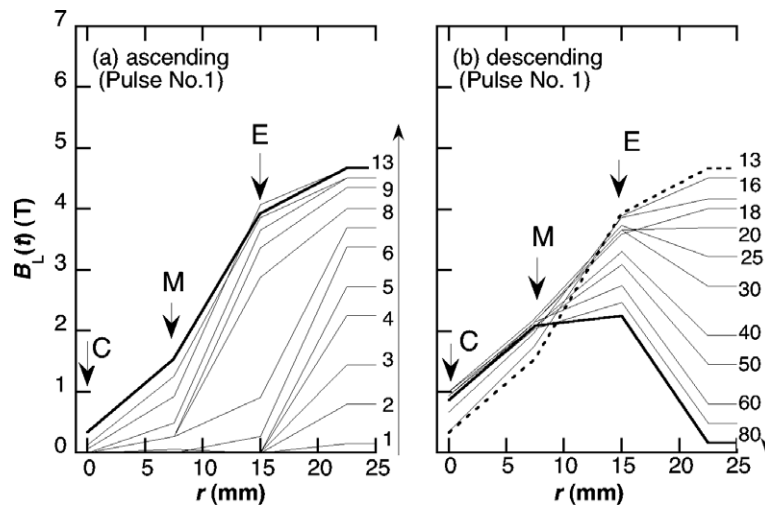
Fig. 2. The time evolution of the local field $B_L(t)$ as a function of the distance along the radius direction for the pulse No. 1 of RUN-1 for the (a) ascending and the (b) descending processes.

the ascending and descending processes, respectively, both of which are reconstructed on the basis of Fig. 1(a). For the ascending process, the flux intrusion starts to increase from the periphery and the small amount of the fluxes arrives at the bulk center. After the $\mu_0 H_a(t)$ value takes a maximum at $t = 13$ ms, the intruded fluxes gradually escape in the region outer than $r = 10$ mm but the local fields at positions C and E continue to increase slightly. If the B_T profile is assumed to be symmetrical along the circumferential direction, it should be noted that the B_T profile for the first stage shows the concave and "*M-shaped*" one. This B_T distribution must be a key point to bring about the trapped field higher than 5 T at the second stage.

Figs. 3(a) and (b) show the similar $B_L(t)$ profile for pulse No. 3 ($B_{ex} = 6.73$ T) of RUN-1 for the ascending and descending processes, respectively. $B_L(E)(t)$ increases but $B_L(C)(t)$ and $B_L(M)(t)$ hardly change for the ascending process. For the descending process, however, $B_L(C)(t)$ sharply increases just after $\mu_0 H_a(t)$ takes a maximum and $B_L(M)(t)$ also slightly increases and the conical trapped field distribution with $B_L(C) > B_L(M) > B_L(E)$ is obtained.

These behaviors suggest that the already trapped fluxes in the first stage are pushed into the bulk center and that the additional fluxes are supplied from the peripheral region. The "*M-shaped*" profile in the first stage changes to the "*cone-shaped*" one at $T_s \sim 30$ K for the pulse No. 3 with $B_{ex} = 6.73$ T. It was pointed out in the previous paper [9] that the height of the cone ($= B_T(C)$) at the second stage depends on the height of the edge in the "*M-shaped*" profile; $B_T(E)$ should be higher and $B_T(C)$ should be lower at the first stage.

Figs. 4(a) and (b) present the time dependences of the applied field and the local fields for RUN-2 and RUN-3 on applying the pulse No. 3, respectively. In RUN-2, where $B_{ex} = 7.01$ T of the pulse No. 3 is higher than that in RUN-1, all the maximum values of local fields, especially $B_L(M)(t)$, increase. Then $B_L(C)(t)$ cannot maintain the higher value and drastically decreases for $t > 60$ ms by a spontaneous flux jump. As a result, the trapped fields at the positions C, M and E decrease to ~ 2 T and the large heat generation should be the origin for the depression. For RUN-3 shown in Fig. 4(b), where lower pulse field
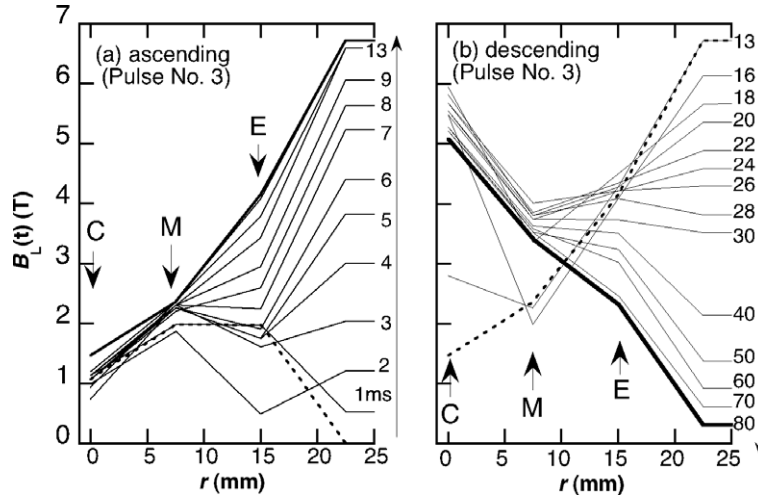
Fig. 3. $B_L(t)$ as a function of the distance along the radius direction on the bulk for the pulse No. 3 of RUN-1 for the (a) ascending and the (b) descending processes.
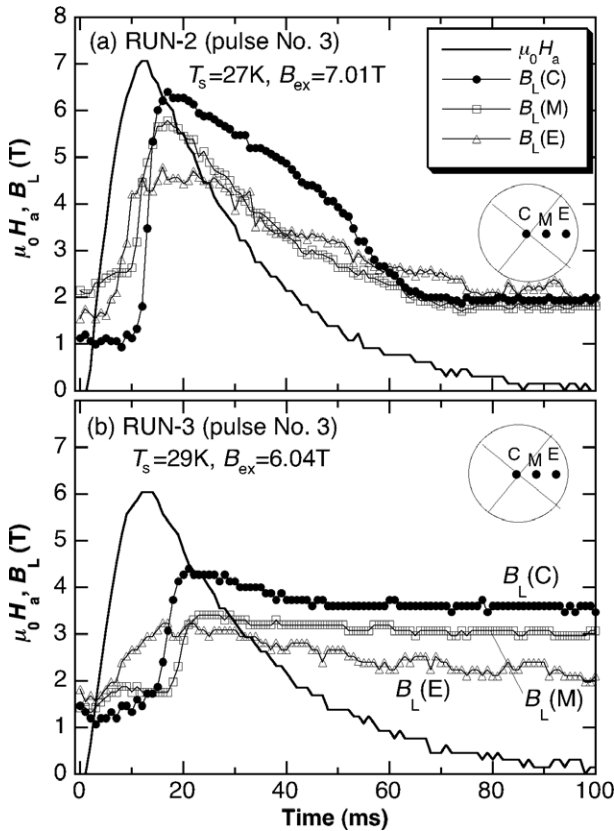

Fig. 4. The time dependences of the applied field and the local fields for (a) RUN-2 and (b) RUN-3 after applying the pulse No. 3.
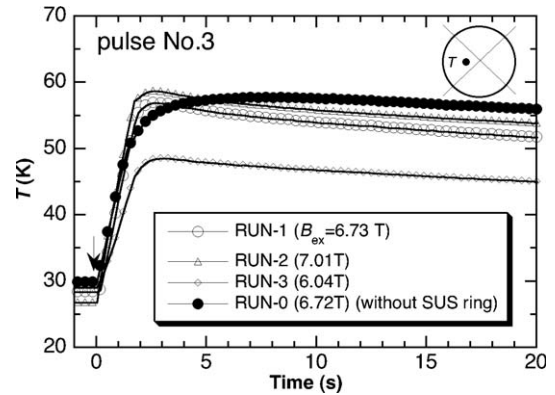

Fig. 5. The time dependences of temperature $T(t)$ at position T after the pulse No. 3 application of each run.

$t = 2$ s and then slowly decreases. The local heat generation and the large temperature rise must mainly occur in the inner part of the bulk within the pulse duration $t \sim 0.1$ s, but the temperature change is observable with a long time delay determined by the thermal diffusivity. The maximum temperature rise ΔT_{max} increases with increasing B_{ex} of the pulse No. 3. $T(t)$ of RUN-0 without stainless steel ring is also shown in Fig. 5 for comparison. It is to be noticed that $T(t)$ for RUN-0 is much different; $T(t)$ slowly increases and takes a maximum at $t \sim 7$ s in spite of the identical ΔT_{max} and T_{max} values to those in RUN-1. These results suggest that the heat propagation changes owing to the metal ring setting and, as a result, the B_T^P is enhanced from 4.47 T to 5.20 T.

In summary, we performed the MMPSC method on the GdBaCuO bulk under several conditions and clarified what are the important factors to enhance B_T^P over 5 T. At the first stage in the MMPSC process, the "*M-shaped*" trapped field profile should be realized on the bulk; $B_T(C)$ at the bulk center should be as low as ~ 1 T and the barrier height $B_T(E)$ at the periphery region must be enhanced to 2.5–3 T.

of $B_{ex} = 6.04$ T was applied, the increase of the $B_L(t)$ at each position is small and the $B_T(C)$ value attains only 3.6 T with a round shaped B_T distribution.

Finally we comment on the effect of the stainless steel ring. Fig. 5 shows the time dependences of temperature $T(t)$ after the pulse No. 3 application of each run. For RUN-1 to RUN-3, $T(t)$ rises up, takes a maximum at

At the second stage at lower T_s, the optimum higher field B_{ex}, which is 6.7 T for this bulk, should be applied. The B_T^P value increased from 4.47 T to 5.20 T as a result of the stainless steel ring setting onto the bulk disk. The microscopic change in the heat propagation should take place by the ring setting onto the bulk. The detailed study is in progress.

References

[1] U. Mizutani, H. Hazama, T. Matsuda, Y. Yanagi, Y. Itoh, K. Sakurai, A. Imai, Supercond. Sci. Technol. 16 (2003) 1207.

[2] Y. Yanagi, Y. Itoh, M. Yoshikawa, T. Oka, T. Hosokawa, H. Ishihara, H. Ikuta, U. Mizutani, in: T. Yamashita, K. Tanabe (Eds.), Advances in Superconductivity XII, Springer-Verlag, Tokyo, 2000, p 47.

[3] H. Fujishiro, K. Yokoyama, T. Oka, K. Noto, Supercond. Sci. Technol. 17 (2004) 51.

[4] H. Fujishiro, M. Kaneyama, K. Yokoyama, T. Oka, K. Noto, Jpn. J. Appl. Phys. 44 (2005) 4919.

[5] H. Fujishiro, K. Yokoyama, M. Kaneyama, M. Ikebe, T. Oka, K. Noto, Physica C 426–431 (2005) 594.

[6] K. Yokoyama, M. Kaneyama, H. Fujishiro, T. Oka, K. Noto, Physica C 426–431 (2005) 671.

[7] H. Fujishiro, M. Kaneyama, T. Tateiwa, T. Oka, Jpn. J. Appl. Phys. 44 (2005) L1221.

[8] H. Fujishiro, K. Yokoyama, M. Kaneyama, T. Oka, K. Noto, IEEE Trans. Appl. Supercond. 15 (2005) 3762.

[9] H. Fujishiro, M. Kaneyama, T. Tateiwa, T. Oka, to be published in J. Phys. Conf. Series (2006).